Effects of Synthetic Jet in Suppressing Cavity Oscillations

S. Sarkar, R. Mandal

Abstract—The three-dimensional incompressible flow past a rectangular open cavity is investigated, where the aspect ratio of the cavity is considered as 4. The principle objective is to use large-eddy simulation to resolve and control the large-scale structures, which are largely responsible for flow oscillations in a cavity. The flow past an open cavity is very common in aerospace applications and can be a cause of acoustic source due to hydrodynamic instability of the shear layer and its interactions with the downstream edge. The unsteady Navier-stokes equations have been solved on a staggered mesh using a symmetry-preserving central difference scheme. Synthetic jet has been used as an active control to suppress the cavity oscillations in wake mode for a Reynolds number of Re_D = 3360. The effect of synthetic jet has been studied by varying the jet amplitude and frequency, which is placed at the upstream wall of the cavity. The study indicates that there exits a frequency band, which is larger than a critical value, is effective in attenuating cavity oscillations when blowing ratio is more than 1.0.

Keywords—Cavity oscillation, Large Eddy Simulation, Synthetic Jet, Flow Control, Turbulence

I. INTRODUCTION

THE flow past a cavity has received a great deal of interest due to its practical applications, for example, in landing systems and weapon bay of aircraft, in the sunroof on cars, in river, lakes or in ship hull. In aerospace, the presence of such cavity may cause huge periodic flow oscillations, which in turn may lead to structural vibrations and production of acute noise. The pressure fluctuations within the cavity can reach up to 170 dB, immensely reducing the stealth capabilities of the aircraft. Further, these may produce environmental hazard due to accumulation of pollutant, denser water or suspended materials in river or canal. The flow oscillations owing to cavities may be beneficial in enhancing heat transfer rates, in most of the cases it is harmful causing vibration and noise as well as increment in drag. Therefore, attenuation of cavity oscillations is very much required.

Cavity flows are characterized by a complex mechanism. The incoming flow separates at the leading edge of the cavity, and forms a shear layer because of the high velocity gradient between the high-speed free stream and the low-speed or even reversed flow in the cavity. The small perturbations are amplified forming vortical structures as a result of Kelvin-Helmholtz (*K-H*) Instability [1]. These vortices roll up and grow as they travel downstream, and violently impinge upon the trailing edge of the cavity generating pressure waves with some phase lag. The pressure waves then travels upstream and adds energy to the forming structures, thus closing the feedback loop and making the process self-sustaining.

S. Sarkar is with the Department of Mechanical Engineering, Indian Institute of Technology Kanpur, Kanpur, 208016, India (phone: +91-9450443556, fax: +91-512 259 7408, e-mail: subra@iitk.ac.in).

R. Mandal is with the Department of Mechanical Engineering, Indian Institute of Technology Kanpur, Kanpur, 208016, India (e-mail: rajib.iitk@gmail.com).

In the literature, this feedback process of cavity oscillations is described as an acoustic phenomenon for high Mach number flows. The cavity oscillations can be classified based on the flow characteristics as shear layer mode and wake mode. In shear layer mode, the shear layer covers the entire length of the cavity, whereas, the shear layer covers half of the length of the cavity in case of wake mode and shedding of vortices occur similar to those behind a bluff body. Periodic oscillations in cavities can be seen over a wide range of Reynolds number, Mach number and also for different combination of length-to-depth ratios. The flow can be considered as laminar, transitional or fully turbulent.

Several experimental and numerical studies have been conducted for flow past a cavity over the last three decades [2]-[6]. It has been shown that, besides the fundamental oscillatory frequency, a number of additional lower frequencies could exist. The energy associated with these modes can be comparable to that of the fundamental oscillatory frequency. It has been also reported that the flow structures originating from a weapon bay at transonic speeds are similar those in an open cavity for incompressible or low Mach number flows [7]. Lately, high resolution numerical schemes such as Direct Numerical Simulation (DNS) [8]-[9], Large-eddy Simulation (LES) [10]-[11] and hybrid RANS/LES [12]-[13] have been used for carrying out cavity flow simulation. Several active and passive control techniques have been used for suppressing cavity oscillations. Passive control methods include spoilers [14], fences [15], rods [16], whereas, steady mass injection [17]-[18], harmonic blowing [19]-[20], piezoelectric actuators and powered resonance tubes have been used as active control in attenuating cavity oscillations. It is seen from the literature that mass injection provides better result than any other control methods. It is also shown by Das et al. [21] that unsteady injection is more effective than steady injection in suppressing oscillations. Stanek et al. [19] have numerically investigated the effect of frequency of pulsed mass injection on the nature of stabilization, destabilization and acoustic suppression in high speed cavity flows. They have considered a wide range of frequencies and found that above a certain frequency level (which they termed as critical frequency), shear layer stabilization was observed, and frequencies below critical level were not effective. Kourta and Vitale [20] have numerically analyzed the control of cavity flow oscillations using synthetic jet actuator and performed an extensive parametric study. They showed that the dynamics of the flow can be modified by properly choosing the amplitude and frequency of the synthetic jet.

Any method that can perturb or change the shear layer may suppress the cavity oscillation. However, this is not trivial. There exist several uncertainties, such as effects of length and time scale of perturbation and how these scales are interacting with the shear layer, effect of blockage or side walls and so on.

The present study uses a LES in resolving the flow structures associated with an open cavity and their interactions with the injected mass flow. We have tried to understand the insight of the flow physics and its control. The effects of synthetic jet have been studied for a wide range of frequencies and blowing ratios. Few issues relating to the effects of length and time scales in perturbing the shear layer and breaking down the coherent structures into small-scale energetic eddies are discussed here.

II. NUMERICAL METHODS

The three-dimensional unsteady filtered Navier-Stokes equations for incompressible flow in the Cartesian coordinate system have been solved, which are:

$$\text{Continuity: } \frac{\partial \overline{u}_j}{\partial x_j} = 0 \tag{1}$$

$$\text{Momentum: } \frac{\partial \overline{u}_i}{\partial t} + \frac{\partial}{\partial x_j}\left(\overline{u}_j \overline{u}_i\right) = -\frac{\partial \overline{P}}{\partial x_i} + \frac{1}{\text{Re}} \nabla^2 \overline{u}_i - \frac{\partial \tau_{ij}}{\partial x_j} \tag{2}$$

Where, u_i represents the velocity field and Re is the Reynolds number. The co-ordinates x, y, z denote the stream wise, wall normal and span wise direction respectively and the corresponding velocities are denoted by u, v and w. The over bar represents the filtered variables and $\tau_{ij} = \overline{u_i u_j} - \overline{u}_i \overline{u}_j$ denotes the subgrid Reynolds stress (SGS) tensor, which represent the effect of subgrid motion on the resolved field of LES. A subgrid-scale model proposed by Germano et al. [22] and modified by Lilly [23] is used to model the SGS stress tensor, where the model coefficient is dynamically calculated instead of input a priori.

The momentum advancement is done explicitly using the second-order Adam-Bashforth scheme, where the pressure term is solved by a standard projection method. The pressure equation is discrete Fourier transformed in one direction (span wise) and is solved by the BI-CG algorithm in the other two directions. The flow solver has been extensively used for variety of transitional and turbulent flows [24]-[26]. The length-to-depth ratio of the cavity considered here is $L/D = 4$, where the flow oscillates in the wake mode. The Reynolds number considered here is $Re_D = 3360$. For the present analysis, a mesh of 392×220×64 is chosen in such a way that there is no appreciable change of flow parameters by further increasing the grid points. The computational domain is shown in Fig. 1. A velocity profile is imposed at inlet, whereas a convective boundary condition is used at the exit with a free slip condition at the upper boundary. A disturbance strip perturbing the wall-normal velocity is imposed at the upstream of the cavity. The synthetic jet is used here as a boundary condition and is placed at the upstream wall of the cavity as shown in Fig. 1. The width of the slot of jet is considered here as $0.25D$. The effects of pulsating jet have been studied for a combination of amplitude and frequency in suppression of cavity oscillations. The amplitude (V_j) of the jet defined as a fraction of U_∞ and are 0.15, 0.6, 0.9 and 1.2 for a fixed frequency of 1320 Hz, which is about three times of predominant vortex shedding frequency. The frequencies of the jet considered here are multiples of dominant vortex shedding frequency without control (f_n) and can be written as $f_j = K f_n$, where, $K = 0.5, 1.5, 2.5, 3.0, 3.5, 4.0, 5.0, 7.0$ and f_n being 440 Hz.
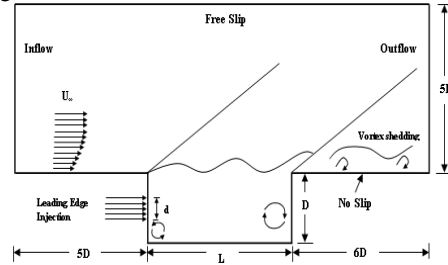

Fig. 1 Computational domain and boundary conditions

The time step used in the present simulation was $\Delta t = 2.0 \times 10^{-3} D/U_\infty$. This time step kept the Courant number below 0.2 for the entire simulation and the viscous stability number was much less. The flow field was allowed to evolve approximately for thirty primary vortex-shedding cycles to get a dynamically steady state solution. Then the data were collected for statistics over further approximately forty cycles, and were found sufficient to ensure statistically converged results.

III. RESULTS AND DISCUSSIONS

LES of flow past rectangular cavities in shear layer mode of oscillation are presented in this section for the sake of validation and are compared against LES data of Chang et al. [10] and experiment of Periera and Sousa [6].

Following the work of Chang et al. [10], A blasius profile with a boundary layer thickness of 0.1D was imposed at the inlet to match the thickness at the upstream edge of the cavity of $L/D = 2$, where Re_D was 3360. This is done following the boundary layer theory [30]. Fig. 2 illustrates the longitudinal mean velocity profile, the resolved normal stresses ($\overline{u'u'}, \overline{v'v'}$) and the shear stress $\overline{u'v'}$ at stations x/D=0.6 and 1.7. The stresses are non-dimensionalized by the inlet free stream velocity. The results of the LES are in good agreement with those of Chang et al. [10]. The profiles at other sections are not shown due to space constraints even though the agreement was good. Fig 2(c) depicts the spectra of the vertical velocity at x/D =1.4. A peak has been observed indicating that the shear layer starts oscillating at the fundamental frequency corresponding to a Strouhal number $St_D = 0.49$. The amplitude of these oscillations is growing in the streamwise direction. Concomitantly, very low-energetic frequency modulations are also observed. According to Rockwell [31], the low frequency components appearing in the spectra can be attributed to the vortex-edge interactions if and only if the energy in these low frequencies is comparable to the main oscillatory frequency. In the present case, the energy associated with these low-frequency oscillations is sensibly smaller than that of the fundamental frequency.

Hence, the low frequency component appearing in this case may be attributed to the influence of recirculation region interacting with the shear layer. The most energetic frequency (St_D = 0.49) at all these stations corresponds to the second mode frequency of $St_D \approx 0.5$ predicted by Rockwell [31] for incompressible flow over a cavity with L/D =2.0. For the second mode, Sarohia [2] measured in his experiments over an axisymmetric cavity a Strouhal number in the range 0.41< St_D <0.49. The same frequency non-dimensionalized with the momentum thickness of the boundary layer at separation is $St_\theta = f\theta/U = 0.015$.
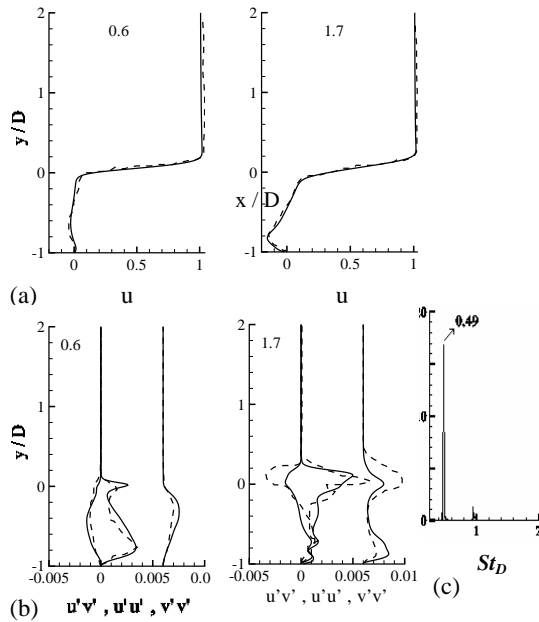
Fig. 2 Comparison of (a) mean velocity profiles, (b) Reynold stress with ---- Chang et al. [7] at X/D = 0.6 and 1.7, (c) velocity spectra at the centre of the cavity

Fig. 3 demonstrates the coupling which takes place between the recirculation region and the shear layer. In shear layer mode, roll up of shear layer vortex occurs *via K-H* instability, and the dynamics of the recirculation region initiates self-sustaining mechanism. The partial clipping of the shear layer is observed in this case. The vortex gets clipped at the trailing edge and convects into the cavity energizing the recirculation region that in turn energizes the shear layer completing the cycle and sustaining the cavity oscillation. The merging of the flow structures arising out of shear layer instability and the concentration of vorticity from the recirculation region (known as pairing) gives rise to the large-scale vortex that later impinges on the downstream cavity edge. As a result, the cavity space is occupied by a primary (larger) eddy and a secondary eddy; the later is close to the separating edge (Fig. 4). The variability of events described here displaying flow oscillations in the shear layer mode, can be attributed to the variety of possible nonlinear interactions in an excited shear layer, mainly by virtue of forcing provided by

the recirculation region and not as a result of pressure waves due to vortex edge interaction.
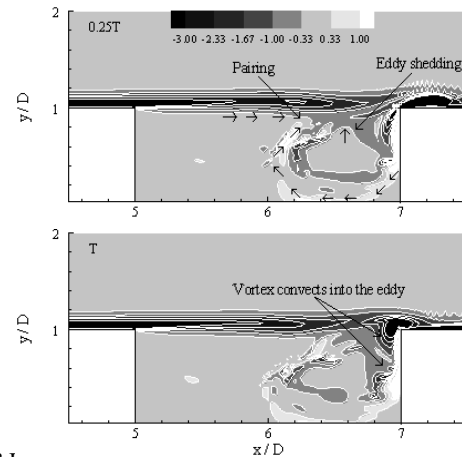

Fig. 3 Instantaneous vorticity contours illustrating pairing and eddy shedding
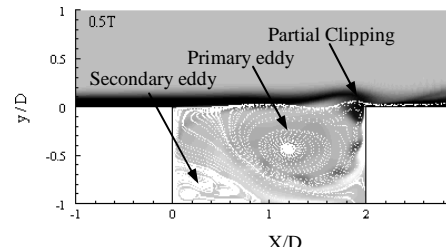

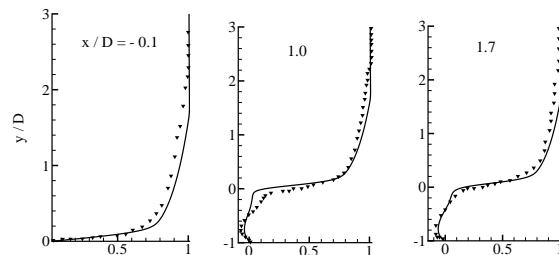Fig. 4 Instantaneous contours of vorticity superimposed with streamlines illustrating recirculation dynamics

Fig. 5 Comparison of mean velocity profiles with experiment of Periera And Sousa [6]
Present LES ———— and experiment ▼▼▼

The experimental data of Pereira and Sousa [6] are now compared with LES results, where the inlet flow was turbulent. The boundary layer thickness and Reynolds number were similar to that used by Pereira and Sousa [6]. Fig 5 shows the comparison of the stream wise mean velocity profile with the experiment at different locations. A good agreement is observed.

A. Vortex Dynamics

The subsequent discussion involves results of LES of flow past a rectangular cavity of *L/D*=4 and suppression of cavity oscillations in the wake mode using synthetic jet at the

upstream wall of the cavity. In this case, a turbulent velocity profile has been used at inlet using the formulation $u/U_\infty = 1-(1- y/\delta)^8$ following Moin et al. [27].

The span wise instantaneous vorticity without control is presented in Fig. 6, which is very illustrative to visualize the flow structure. In case, initial roll up of shear layer occurs *via K-H* instability and shedding of these vortices takes place similar to that behind a bluff body. After formation of vortices, they get energized due to non-linear interactions and convect downstream impinging on the trailing edge of the cavity. Then the vortex loses its integrity giving rise to changes in concentration of vorticity associated with sudden changes in velocity and pressure. These sudden changes in flow parameters i.e. disturbances (may be called pressure waves), generated at the impingement edge, travel upstream and adds energy to the growing instabilities in the shear layer sustaining the oscillations (visible in the Fig.). The cavity shear layer appears as three half waves indicating the third mode of oscillations according to Gharib and Roshko [28]. Here, we observe partial clipping of the shear layer vortex as termed by Rockwell and Kinsley [29].
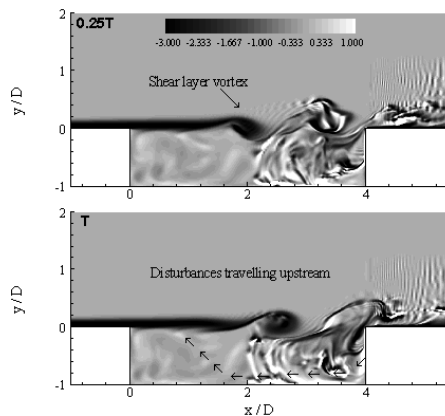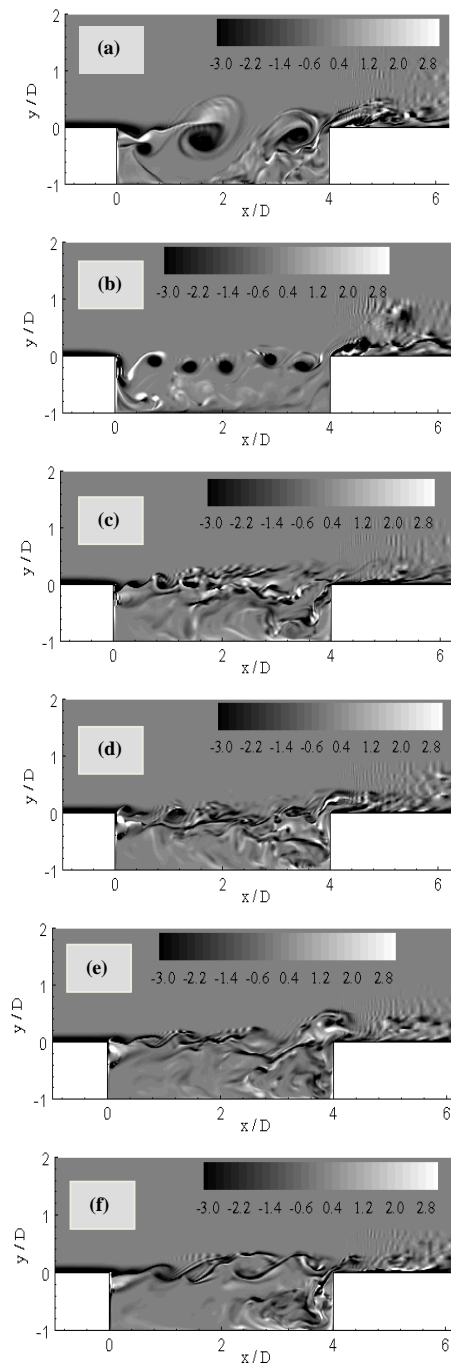

Fig. 6 The instantaneous vorticity contours illustrating vortex-edge interaction in the wake mode, $L/D = 4$

Vortex dynamics with pulsating injection for a wide range of frequencies depicting suppression of cavity oscillations are presented in Fig 7 for a fixed amplitude, $V_J = 1.2$. What is interesting to note that the flow structures and associated vortex dynamics change significantly with frequency of pulsating jet. The cavity are occupied with two significant larger vortices with pulsating jet having frequency $f_j = 220$ Hz, which is half of the dominant vortex shedding frequency without injection, causing a detrimental effect. The flow pattern has utterly changed with pulsating jet of $f_j = 660$ Hz.

Here, the shear layer has been broken to relatively smaller but ordered vortices and the cavity is occupied with five prominent rolls with partial escape of vortices. As the frequency of synthetic jet is increased to 1100 Hz, the shear layer breaks down into small-scale eddies illustrating usefulness of synthetic jet. The similar flow pattern prevails with appearance of abundant energetic small-scale eddies along with the coherent structures as the frequency is further increased.

However, there exists some difference in flow structures in minute details. For the frequency $f_j = 2200$ Hz, stabilization of shear layer is very apparent. The flow visualization illustrates that the pulsating jet having frequency $f_j > 1100$ Hz (two and half times of the dominant vortex shedding frequency), is effective in breaking the large-scale structure and thus attenuating cavity oscillations. Although the above discussion is qualitative, it give us a fair idea that how the system is sensitive with the frequency of external perturbation.
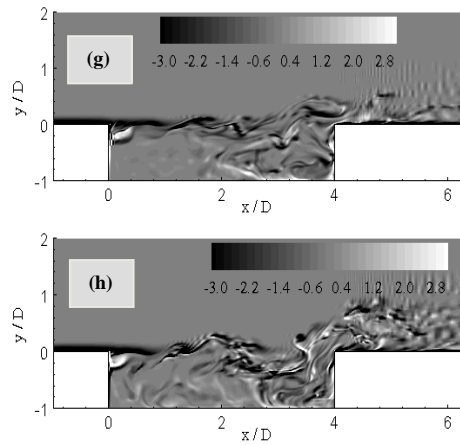
Fig. 7 Instantaneous vorticity contours with different frequency of pulsating jet: (a) 220 Hz, (b) 660 Hz, (c) 1100 Hz, (d) 1320 Hz, (e) 1540 Hz, (f) 1760 Hz, (g) 2200 Hz and (h) 3080 Hz
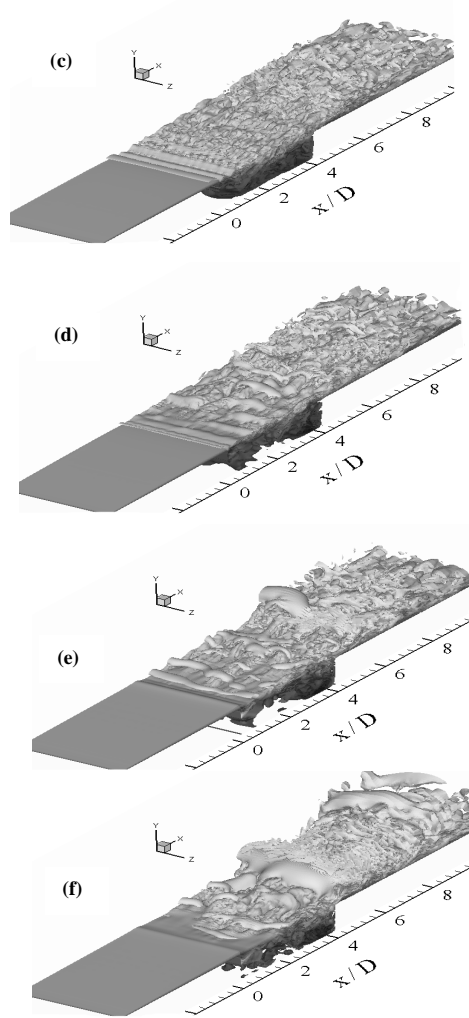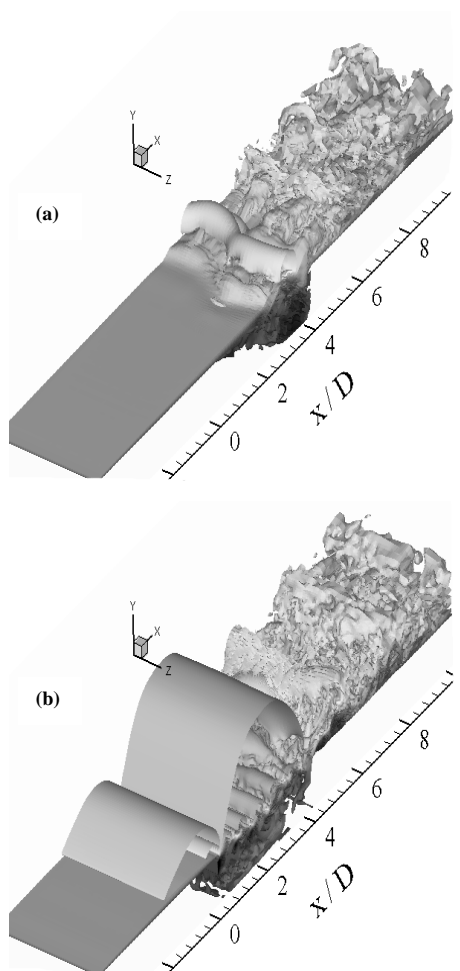

Fig. 8 Instantaneous spanwise velocities: (a) without control, (b) 660 Hz, (c) 1100 Hz, (d) 1540 Hz, (e) 1760 Hz and (f) 3080 Hz

The iso-surface of streamwise component of instantaneous velocity has been shown in Fig. 8 to illustrate the three-dimensional flow structures. The roll up of the shear layer, its span wise distortion and then breaking down to turbulent flow after impingement can be seen, Fig 8a (without control). Appearance of large-scale coherent structure from rollup of shear layer prevails up to $f_j = 660$ Hz. For higher frequency ($f_j \geq 1100$ Hz), the breakdown of shear layer is observed from the beginning with appearance of longitudinal streaks and hairpin vortices that eventually evolve to a turbulent shear layer. Experiment of Kiya and Sasaki [32], DNS of Na and Moin [33] confirm the existence of hairpin vortices in the separated flow region. Thus, Fig 8 elucidates the effectiveness of pulsating jet in attenuating cavity oscillations, although augmentation of turbulence from the beginning may be evident.
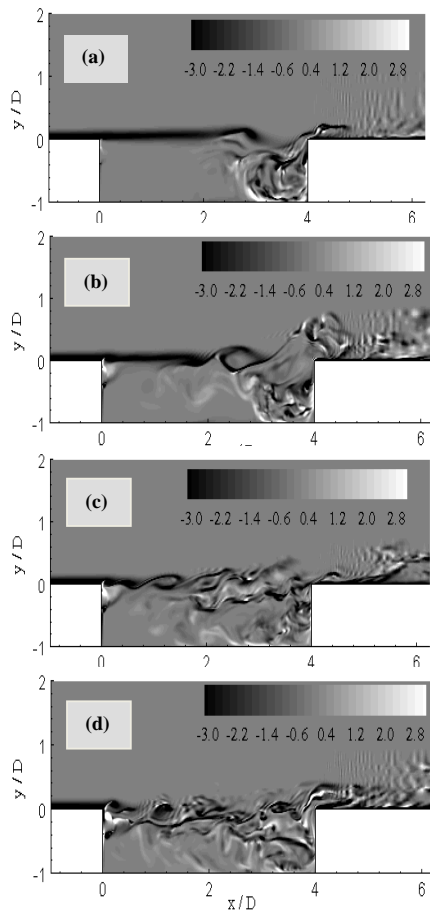
Fig. 9 Instantaneous vorticity contours for different amplitude of pulsating jet: (a) 0.15, (b) 0.6, (c) 0.9 and (d) 1.2

The effect of amplitude of injection has been studied for varying blowing ratio 0.15, 0.6, 0.9 and 1.2 with a fixed frequency of 1320 Hz, which is about three times of predominant vortex shedding frequency. From the instantaneous vorticity contours (Fig. 9), it is seen that that the large-scale coherent vortices developed due to the instability of shear layer, which are responsible for cavity oscillations, have not been attenuated for amplitude 0.15 and 0.6. A partial clipping is observed for those cases. As amplitude of synthetic jet is increased to 0.9 and to further 1.2, the shear layer is progressively characterized by appearance of high frequency small-scale eddies. The coherent vortices found for amplitude of 1.2 do not have considerable strength thus attenuating cavity oscillations. Thus considering the vortex dynamics, it appeared that amplitude greater than 1 is effective in suppression of cavity oscillations when frequency $f_j > 1100$ Hz.

B. Velocity Spectra

The vertical velocity spectra without any control presented in Fig. 10 for two representative locations at $x/D = 1.5$ and 2.5 (where, the leading edge of the cavity is considered as origin)

display a spectrum with energetic frequencies up to strouhal number of $St_D < 1.0$. The energy amplification of separated shear layer within the cavity is not the same for the main energetic frequencies. At the location $x/D = 1.5$, a peak in the velocity spectrum is observed to occur at $St_D = 0.44$ indicating the dominant vortex shedding frequency. At $x/D = 2.5$, a second energetic frequency of $St_D = 0.25$ has been observed along with other low-energetic frequency components, which can be attributed to the interaction of the shear layer vortex with the trailing edge. It is noted that these low-energetic frequency oscillations other than the dominant frequency were not present in shear layer mode. The maximum amplitude of oscillations corresponding to the vortex shedding frequency at $x/D = 2.5$ is 6.6.
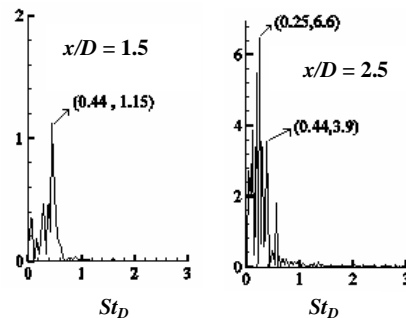

Fig. 10 Velocity spectra at two locations without control

To illustrate the effect of control in attenuating cavity oscillation the spectral analysis has been performed. Here the velocity and pressure signals are collected for about thirty vortex shedding cycles after the dynamic stability for different combinations of amplitude and frequency. The velocity spectra at x/D = 2.5 for varying blowing ratios i.e. (a) 0.15, (b) 0.6, (c) 0.9 and (d) 1.2 are shown in Fig. 11 for a frequency of 1320 Hz. The dominant non-dimensional frequency is 0.44 for without control, whereas, it is 0.4, 0.36, 0.6 and 0.22 for V_j= 0.15, 0.6, 0.9 and 1.2 respectively. In terms of amplitude of oscillations, it is 6.6 for no control, but for other cases, it is 39.10, 17.6, 5.54 and 1.24 respectively. This illustrates that synthetic jet is very effective in suppressing the cavity oscillations for amplitude of 1.2.
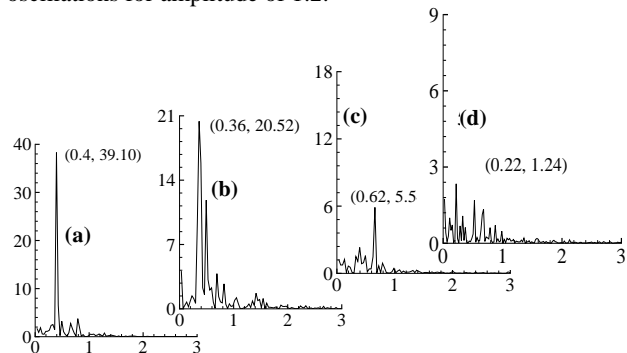

Fig. 11 Vertical velocity spectra at $X/D = 2.5$ for different amplitude: (a) 0.15, (b) 0.6, (c) 0.9 and (d) 1.2

Fig. 12 depicts the spectra of vertical velocity for different frequency with a fixed amplitude V_j= 1.2 at the same location x/D = 2.5 to demonstrate the response of frequency in suppressing the cavity oscillations. The energy amplification of separated shear layer occurs at frequency St_D = 0.22, 0.33, 0.18, 0.22, 0.5, 0.7, 0.62 and 0.26 when the imposed f_j = 220, 660, 1100, 1320, 1540, 1760, 2200 and 3080 Hz respectively. The corresponding amplitudes of oscillations for these energetic frequencies are 53, 72, 15, 1.24, 1.6, 2.54, 5.5 and 5.6. It is note worthy that for low values of frequency (frequency up to 660Hz with pulsating jet in the present case), when the cavity flow is characterized by the appearance of large-scale coherent structures, the energetic frequencies appears as the sub-frequency of the imposed frequency. There is no relation between the frequency of the synthetic jet and the energetic frequency after a certain range. This points toward the existence of a critical frequency above which the shear layer is dominant with small-scale eddies suppressing the cavity oscillation. Although, to accurately predict the critical frequency further analyses are needed. However, the present results clearly depicts that for frequency f_j >1100, a band of energetic frequencies exit illustrating the breakdown of coherent structures. The spectral analyses resolve that the pulsating jet with frequency larger than a certain value, in this case f_j >1100 Hz, which may be called critical frequency, is effective in attenuation of cavity oscillations.
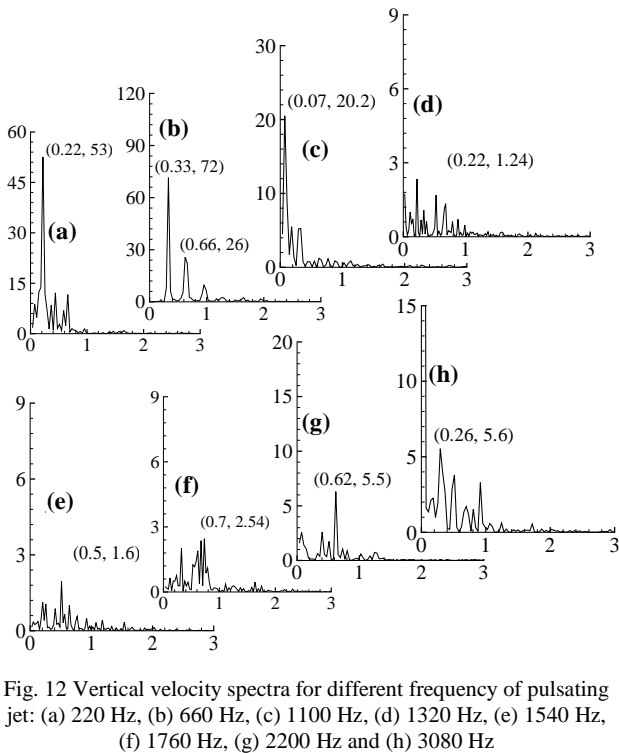

Fig. 12 Vertical velocity spectra for different frequency of pulsating jet: (a) 220 Hz, (b) 660 Hz, (c) 1100 Hz, (d) 1320 Hz, (e) 1540 Hz, (f) 1760 Hz, (g) 2200 Hz and (h) 3080 Hz

C. Turbulent Kinetic Energy

The evolution of turbulent kinetic energy (TKE) for varying blowing ratio and frequency of pulsating jet at four stations are shown in Fig. 13 and 14.

It has been observed that the TKE is concentrated along the shear layer over the first half of the cavity and its value increases with blowing ratio, Fig. 13. However, TKE does not grow in the second half and even decreases as compared to without any mass injections. This illustrates the reduced vortex-edge interaction because of breaking down of shear layer for larger blowing ratio, particularly when it is more than 0.9.

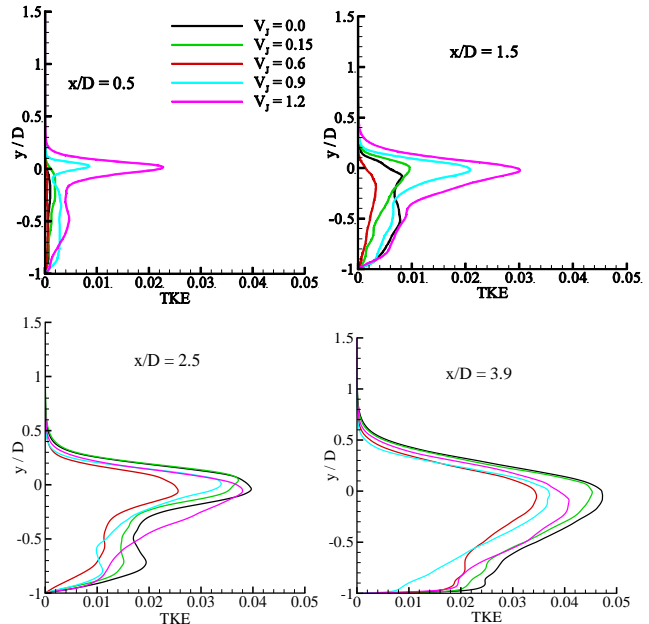

Fig. 13 TKE profiles within the cavity for varying blowing ration of pulsating jet for a fixed frequency, 1320 Hz
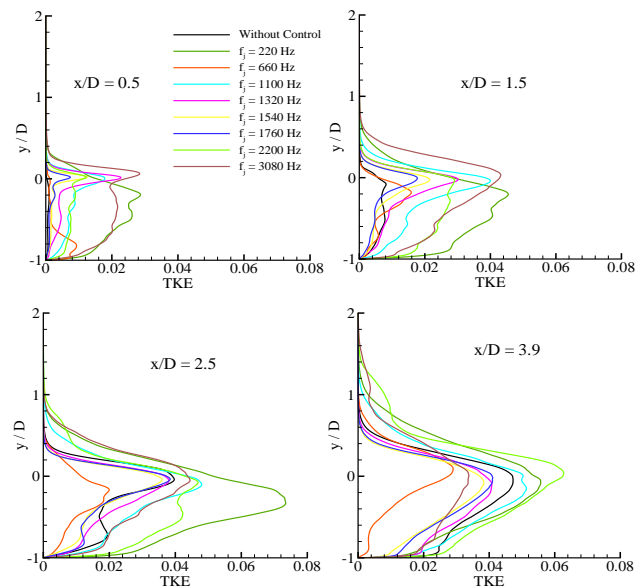

Fig. 14 TKE profiles within the cavity for varying frequency of pulsating jet for a fixed blowing ratio, 1.2

The turbulent kinetic energy (TKE) profiles for varying frequency of pulsating jet at four stations presented in Fig. 14, exhibit the similar trend. TKE is higher with mass injection than that of clean flow at the first half of the cavity particularly for low frequency pulsating jet attributing to the appearance of large-scale vortices. However, in the second half of the cavity, TKE tends to decrease with pulsating jet of $f_j = 660$ to 1760 Hz and is even lower in magnitude than that of without control illustrating the breakdown of shear layer and the attenuation of vortex-edge interaction.

IV. CONCLUSION

The three-dimensional incompressible flow past an open cavity in the wake mode of oscillations for a Reynolds number of $Re_D = 3360$ and a length-to-depth ratio of $L/D = 4$ has been analyzed using LES. A pulsating jet for different combinations of amplitude and frequency has been used to suppress the cavity oscillation. The present LES is successful in resolving the large-scale structures, which are responsible for cavity oscillations. In the wake mode, the roll up of shear layer initiates via *K-H* instability, perturbations from the trailing edge as a result of vortex-edge interactions travel upstream and energize the forming structures sustaining the cavity oscillation, where the flow is characterized by low-frequencies large-scale eddies.

Vortex dynamics illustrates that flow structure noticeably changes with the amplitude and frequency of pulsating jet. The shear layer breaks down to energetic small-scale eddies for frequencies larger than two and half times of fundamental vortex shedding frequency of the cavity when the blowing ratio is more than 1.0. Spectral analyses also support that unsteady injection is effective in suppression of cavity oscillations above a certain level of frequency (may be called critical frequency), which is 1100 Hz in the present case. The turbulence levels increases in the beginning, however in the second half of the cavity, turbulence generated is less than that of without injection illustrating annihilation of vortex-edge interaction, particularly in the range of $2.5 f_n \leq f_j \leq 4.0 f_n$ and $V_J > 1.0$.

TABLE I
NOMENCLATURE

Symbol	Quantity
D	Depth of cavity
L	Length of the cavity
Re_D	Reynolds number based on the cavity depth
St_D	Strouhal number based on cavity depth
U_∞	Free stream velocity
V_j	Amplitude of synthetic jet
d	Width of the slot of jet
f_j	Frequency of synthetic jet

REFERENCES

[1] G. Ashcroft and X. Zhang, "Vortical Structures over Rectangular Cavities at Low speed," Physics of Fluids, vol.17, No.1, pp. 015104-1—015104-8, 2005.

[2] V. Sarohia, "Experimental investigation of oscillations in flows over shallow cavities," AIAA Journal, vol.15, pp. 984-991, 1977.

[3] D. Rockwell and E. Naudascher, "Review—Self-sustaining oscillations of flow past cavities," ASME Journal of Fluids Engineering, vol.100, pp. 152-165, 1978.

[4] D. Rockwell and C. Knisely, "Observation of the three-dimensional nature of unstable flow past a cavity," Physics of Fluids, vol.23, pp. 425-431, 1980.

[5] J. C. F. Pereira and J. M. M. Sousa, "Influence of impingement edge geometry on cavity flow oscillations," AIAA Journal, vol.32, pp. 1737-1740, 1994.

[6] J. C. F. Pereira and J. M. M. Sousa, "Experimental and numerical investigation of flow oscillations in a rectangular cavity," ASME Journal of Fluids Engineering, vol.117, pp. 68-73, 1995.

[7] C. W. Rowley, T. Colonius and A. J. Basu, "On self-sustained oscillations in two-dimensional compressible flow over rectangular cavities," Journal of Fluid Mechanics, vol.455, pp. 315-346, 2002.

[8] A. Hamed, D. Basu, D. Mohamed and K. Das, "Direct Numerical Simulations of High Speed Flow over Cavity," Proceedings (TAICDL), August 5-9, 2001.

[9] T. Colonius, A. J. Basu and C. W. Rowley, "Numerical Investigation of the Flow Past a Cavity," AIAA Paper, 99-1912, 10-12 May, 1999.

[10] K. Chang, G. Constantinescu and S. O. Park, "Analysis of the flow and mass transfer processes for the incompressible flow past an open cavity with a laminar and a fully turbulent incoming boundary layer," Journal of Fluid Mechanics, vol.561, pp. 113-145, 2006.

[11] D. P. Rizzetta and M. R. Visbal, "Large Eddy Simulation of Supersonic Cavity Flow fields Including Flow Control," AIAA Paper, 2002-2853, 24-26 June, 2002.

[12] S. Arunajatesan, J. D. Shipman and N. Sinha, "Hybrid RANS-LES Simulation of Cavity Flow Fields with Control," AIAA Paper, 2002-1130, 14-17 January, 2002.

[13] D. Basu, A. Hamed and K. Das, "DES and Hybrid RANS/LES models for unsteady separated turbulent flow predictions," AIAA Paper, 2005-0503, 10-13 January, 2005.

[14] M. E. Franke and R. Sarno, "Suppression of Flow Induced Pressure Oscillations in Cavities," AIAA Paper, 90-4018, October 1990.

[15] S. McGrath and L. Shaw, "Active Control of Shallow Cavity Acoustic Resonance," AIAA Paper, 96-1949, 17-20 June, 1996.

[16] M. J. Stanek, J. A. Ross, J. Odedra and J. Peto, "High Frequency Acoustic Suppression-The Mystery of the Rod-in-Crossflow Revealed," AIAA Paper, 2003-0007, 6-9 January, 2003.

[17] A. D. Vakili and C. Gauthier, "Control of Cavity Flow by Upstream Mass-Injection," Journal of Aircraft, vol.31, No.1, pp. 169-174, 1994.

[18] V. Suponitsky, E. Avital and M. Gaster, "On three-dimensionality and control of incompressible cavity flow," Physics of Fluids, vol.17, pp. 104103-1—104103-19, 2005.

[19] M. J. Stanek, M. R. Visbal, D. P. Rizzetta, S. G. Rubin and P. K. Khosla, "On a mechanism of stabilizing turbulent free shear layers in cavity flows," Computers & Fluids, vol.36, pp. 1621-1637, 2007.

[20] A. Kourta and E. Vitale, "Analysis and control of cavity flow," Physics of Fluids, vol.20, pp. 077104-1--077104-10, 2008.

[21] K. Das, A. Hamed and D. Basu, "Numerical Investigations Of Transonic Cavity Flow Control Using Steady And Pulsed Fluidic Injection," Proceedings of FEDSM 2005-77422, ASME FEDSM, 19-23 June, 2005.

[22] M. Germano, U. Piomelli, P. Moin and W. H. Cabot, "A dynamic subgrid-scale eddy viscosity model," Physics of Fluids A, vol.3, pp. 1760-1765, 1991.

[23] D. K. Lilly, "A proposed modification of the Germano subgrid-scale closure method," Physics of Fluids A, vol.4, pp. 633-635, 1992.

[24] S. Sarkar and P. R. Voke, "Large-eddy simulation of unsteady surface pressure on a LP turbine blade due to interactions of passing wakes and inflexional boundary layer," ASME Journal of Turbomachinery, vol.128, pp. 221-231, 2006.

[25] S. Sarkar, "Identification of flow structures on a LP turbine blade due to periodic passing wakes," ASME Journal of Fluids Engineering, vol.130, pp. 061103-1--061103-10, 2008.

[26] S. Sarkar and Sudipto Sarkar, "Large-Eddy Simulation of Wake and Boundary Layer Interactions behind a Circular Cylinder," ASME Journal of Fluids Engineering, vol.131, pp. 091201-1—091201-13, 2009.

[27] P. Moin and J. Kim, "On the numerical solution of time dependent viscous incompressible fluid flows involving solid boundaries," Journal of Computational Physics, vol.35, pp. 381-392, 1980.

[28] M. Gharib and A. Roshko, "The effect of flow oscillations on cavity drag," Journal of Fluid Mechanics, vol.177, pp. 501-530, 1987.

[29] D. Rockwell and C. Knisely, "Vortex-edge interaction: Mechanism for generating low frequency components," Physics of Fluids, vol.23, No.2, pp. 239-240, 1979.

[30] H. Schlichting, "Boundary Layer Theory", 7th Edition, McGraw-Hill Book Co, New York (1979).

[31] D. Rockwell, "Prediction of oscillation frequencies for unstable flow past cavities", *Journal of Fluids Engineering*, Vol. 99, pp 294–300, 1977.

[32] M. Kiya and K. Sasaki, "Structure of large-scale vortices and unsteady reverse flow in the reattaching zone of a turbulent separation bubble", *Journal of Fluid Mechanics*, Vol. 154, pp. 463-491, 1985.

[33] Y. Na and P. Moin, "Direct Numerical Simulation of a separated turbulent boundary layer", *Journal of Fluid Mechanics*, Vol. 374, pp. 379-405, 1998.

S. Sarkar, Professor of the Department of Mechanical Engineering at the Indian Institute of Technology Kanpur, India and a member of the American Society of Mechanical Engineers (ASME), received his Bachelor degree in Mechanical Engineering from the University of Calcutta, India and Master degree from Indian Institute of Science, Bangalore and PhD from Indian Institute of Technology, Madras. He served the University of Calcutta from 1988 to 1997 and then moved to Indian Institute of Technology, Kanpur. He visited the University of Surrey, UK as a senior research fellow in 2001 for two years. His research interest is mainly centered on Turbomachinery, CFD, Fluid Mechanics and Turbulence. He is the author of about 80 technical papers in international journals and conferences, and has guided several masters and doctoral students.

R. Mandal received his Bachelor degree in Mechanical Engineering from Bengal Engineering and Science University, Shibpur, 2009, and Master degree from Indian Institute of Technology, Kanpur, 2011. At present, he is working as Research Associate in the Department of Mechanical Engineering at the Indian Institute of Technology Kanpur. His research interest is in CFD, Fluid Mechanics and Heat Transfer.